Precise diffraction efficiency measurements of large-area greater-than-99%-efficient dielectric gratings at the Littrow angle

Patrick P. Lu,[1] Ke-Xun Sun,[1,*] Robert L. Byer,[1] Jerald A. Britten,[2] Hoang T. Nguyen,[2] James D. Nissen,[2] Cindy C. Larson,[2] Michael D. Aasen,[2] Thomas C. Carlson,[2] and Curly R. Hoaglan[2]

[1]*Ginzton Laboratory, Stanford University, 450 Via Palou, Stanford, California 94305-4088, USA*
[2]*Lawrence Livermore National Laboratory, Livermore, California 94550, USA*
[*]*Corresponding author: kxsun@stanford.edu*

Received February 24, 2009; revised April 17, 2009; accepted April 26, 2009; posted April 29, 2009 (Doc. ID 108010); published May 28, 2009

We have developed improved cavity-finesse methods for characterizing the diffraction efficiencies of large gratings at the Littrow angle. These methods include measuring cavity length with optical techniques, using a Michelson interferometer to calibrate piezoelectric transducer nonlinearities and angle-tuning procedures to confirm optimal alignment. We used these methods to characterize two 20 cm scale dielectric gratings. The values taken from across their surfaces collectively had means and standard deviations of $\mu = 99.293\%$ and $\sigma = 0.164\%$ and $\mu = 99.084\%$ and $\sigma = 0.079\%$. The greatest efficiency observed at a single point on a grating was $(99.577 \pm 0.002)\%$, which is also the most accurate measurement of the diffraction efficiency in the literature of which we are aware. These results prove that a high diffraction efficiency with low variation is achievable across large apertures for gratings. © 2009 Optical Society of America © 2009 Optical Society of America

OCIS codes: 050.1950, 120.2230, 120.3180, 230.1360.

Grating-based interferometers have been proposed as candidates for future development beyond current Laser Interferometer Gravitational Wave Observatory (LIGO) and Laser Interferometer Space Antenna (LISA) baselines [1,2]. All-reflective grating interferometers eliminate volumetric transmissive heating and enable a wider selection of materials with such desired properties as higher mechanical Q and thermal conductivity, thereby enabling high power for high sensitivity and simpler interferometer architecture. We have demonstrated grating interferometers using overcoated metal gratings [1], studied their thermal loading properties [3,4], and contemplated the use of dielectric gratings [5]. Recently, centimeter-scale dielectric gratings were used and characterized in interferometers [6,7].

Advanced LIGO calls for transmissive optics with diameters up to 34 cm [8]. For future grating interferometers beyond advanced LIGO, apertures as large as 1 m may be required, depending on grating groove density and interferometer configuration. Large-aperture dielectric gratings are a key challenge for realizing grating interferometers in future gravitational wave detectors. A viable source of these may be to leverage large-area dielectric gratings developed for chirped-pulse amplification in petawatt-class laser systems, for which significant work has already been done in modeling and fabrication [9–11].

The ability to make precise diffraction efficiency measurements is essential to meeting the performance goals of interferometers that use gratings. Cavity-finesse measurements have previously been demonstrated to accurately determine grating diffraction efficiency at the Littrow angle [7]. With proper alignment and vibration control, this method attains high sensitivity, because the diffraction efficiency is sampled on each round trip of the light in the cavity. A high-finesse cavity also rejects any small-angle scattering that might exist in a direct single-pass measurement of the diffraction efficiency.

We tested two HfO_2/SiO_2 multilayer dielectric (MLD) gratings: one is 200 mm × 100 mm and the other is 170 mm × 100 mm in size. These were fabricated at the Lawrence Livermore National Laboratory (LLNL) using holographic exposure followed by ion-beam etching to transfer the grating pattern into the top SiO_2 layer. They were representatives of larger gratings made with the same process, with gratings of up to 910 mm × 450 mm having been made. The groove density was 1740 lines/mm.

The diffraction efficiency at the first order Littrow angle was measured at the LLNL using scanning photometry, which measured light returning from a single pass off the grating. An automated scanning photometer, illustrated in Fig. 1(a), translated the gratings along two axes while illuminating them with TE-polarized light at 1064 nm. The returning light was separated from the beam path with a beam splitter and collected in an integrating sphere. The calibration of the apparatus was periodically verified using a highly reflective (HR) mirror of known reflectance.

To obtain a more precise measurement of the diffraction efficiency, we constructed a cavity-finesse experiment, shown schematically in Fig. 1(b). For this, we illuminated an $\mathcal{F} = 50$ mode cleaner cavity with 1064 nm light from a nonplanar ring oscillator (NPRO) laser. The mode cleaner was a nondegenerate ring resonator that improved the spatial profile of the beam for a better mode matching into our grating cavity. It was locked with 12 MHz sidebands that were of sufficient amplitude to serve as frequency ref-

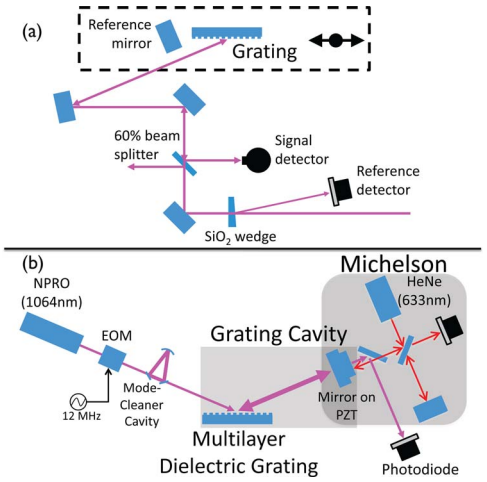

Fig. 1. (Color online) (a) Setup for scanning photometry measurements. (b) Experimental setup for the cavity-finesse method.

erences for the grating cavity under test. Our cavity consisted of a grating and an HR end mirror placed at the grating's first order Littrow angle. The mirror mount contained a three-point piezo adjuster, enabling cavity length actuation and fine angular adjustments. We custom modified the mirror and grating mounts for greater weight and damping to enhance cavity rigidity. TE-polarized light was coupled into the cavity through specular reflection off the grating, and light escaping through the end mirror was monitored as the cavity length was sinusoidally scanned as a function of time. Sinusoidal mirror actuation was chosen to suppress potential ringing in the piezoelectric transducer (PZT).

To calibrate for the sinusoidal drive voltage and nonlinearities in the piezo, we used a Michelson interferometer to observe the position and the speed of the cavity end mirror. A He–Ne laser at 633 nm was used as the source, and the phase of the reflected light from the back of the end mirror was monitored at the output port of the interferometer.

For each grating, the finesse was measured at points taken from two regularly spaced grids of different sizes. A larger grid spanned the entire grating surface, and a smaller grid covering a 4.5 mm spot at the center of the grating quantified local variations.

Figure 2(a) shows a diffraction efficiency map of the 200 mm $\times$ 100 mm grating comprising 15 k points obtained by scanning photometry. These points were measured to have an average efficiency of $\mu=99.2\%$ and a standard deviation of $\sigma=0.3\%$. Figure 2(b) shows the measured finesse of this grating, taken from a 5×3 grid across the surface and converted into the diffraction efficiencies. These points had $\mu=99.293\%$ and $\sigma=0.164\%$. A 4.5 mm spot at the center of the grating was measured with a 3×3 grid, resulting in an average value of $\mu=99.414\%$ and a standard deviation of $\sigma=0.097\%$. For the 170 mm $\times$ 100 mm grating, a 4×3 grid extending over the entire surface yielded values of $\mu=99.084\%$ and $\sigma=0.079\%$, and a 4.5 mm spot from the grating center had $\mu=99.139\%$ and $\sigma=0.041\%$.

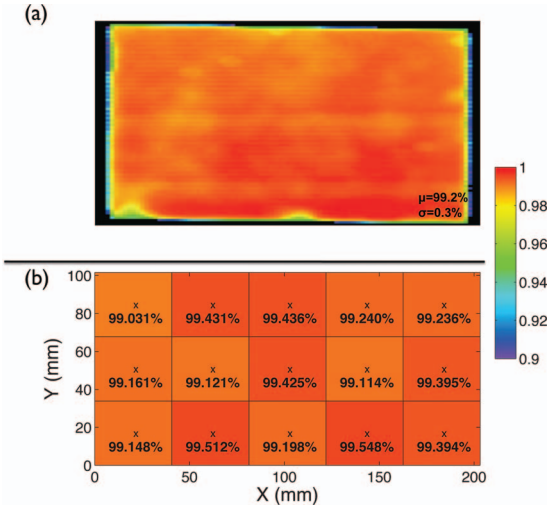

Fig. 2. (a) Diffraction efficiency map, as measured by scanning photometry. (b) Diffraction efficiency measured over a 5×3 grid using the cavity-finesse technique.

Next, we detail the procedure used for measuring the finesse. The figures and numbers used in the text are for the point on the grating with the highest observed diffraction efficiency.

The free spectral range (FSR) was determined by observing cavity transmission during a scan of the cavity length and measuring the physical actuation distance between the carrier and sideband transmission peaks. This reveals the ratio between scan distance and frequency and thus the cavity size. The cavity transmission contained interference terms between the carrier and the sidebands at 12 MHz as well as between opposing sidebands at 24 MHz. A low-pass filter removes these beating terms and reveals the underlying Lorentzian line shape of the cavity transmission, plotted in Fig. 3. A calibrated length scale, made possible by the Michelson interferometer, is used as the x axis and confirms that adjacent carrier peaks were spaced at half the 1064 nm wavelength, as seen in Fig. 3(a). We scanned at 37 Hz. This frequency was picked to avoid acoustic distortions that might have occurred during the time of traversal from peak to peak but is still slow enough that cavity dynamics did not significantly distort the

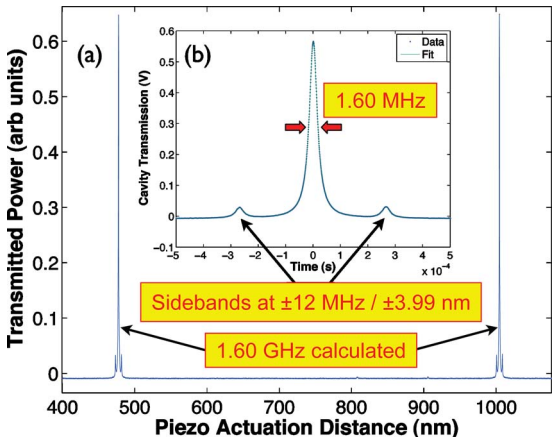

Fig. 3. (Color online) (a) Cavity transmission versus piezo actuation. (b) Transmission peak and sidebands.

Lorentzian line shape of the carrier and sidebands. A least-squares fit of the carrier and the sideband peaks to three summed and shifted Lorentzians determines the sideband and the carrier peak locations. In this example, the distance of the sidebands from the carrier was 3.986 ± 0.006 nm, which corresponds to an FSR of 1.601 ± 0.003 GHz or a cavity length of 93.6 ± 0.2 mm. The measured value for sideband spacing is averaged from 20 samples. Using this cavity length and the mirror curvature of 30 cm, the radii of the beam are calculated to be 217 and 262 μm on the grating and the mirror, respectively.

When measuring the FWHM of the cavity peaks, we used a slower scan rate, dwelling roughly 1 ms over a peak and its sidebands, as seen in Fig. 3(b). The measurement duration was short enough to reject environmental acoustics but long enough to avoid transient effects, thus ensuring that the steady-state formulas for cavity transmission were valid. Again, a triple-Lorentzian fit is performed. This measures the center peak width to be 1.597 ± 0.003 MHz by comparing the center peak to the sideband spacing. We used a sample size of 10. The finesse is thus calculated to be 1002 ± 3. The dwell time over the FWHM region of the peak was 36 μs, which was 364 times the cavity lifetime, well within the steady-state regime.

To determine the reflectivity of the cavity end mirror, two other unknown mirrors were used. Between the three mirrors, three different pairings making three different cavities were possible, and we measured the finesse of each in turn. With these three measurements, we were able to determine the reflectivity of all three mirrors. The end mirror used to form the grating cavities had a reflectivity of $(99.797 \pm 0.001)\%$, consistent with transmittance measurements made by the vendor. Using this value, the diffraction efficiency is calculated to be $(99.577 \pm 0.002)\%$.

Since cavity misalignments induce round-trip losses, they can reduce the measured diffraction efficiency. During our measurement of peak widths, we tuned the alignment of the end mirror using a three-axis piezo mirror mount. The x axis was first adjusted in increments of 4.7 μrad. When the highest finesse was found, a similar procedure optimized the y axis.

The zeroth order transmission and reflection were measured to be 1.2×10^{-4} and 1.0×10^{-3}, respectively. This puts the upper limit on absorption and scattering at 0.31%.

To conclude, we have measured the diffraction efficiencies at the Littrow angle of two large-area dielectric gratings using the cavity-finesse method. Each point was over 99% efficient, amply exceeding the current requirements for the advanced LIGO arm cavities, which are baselined at 450 finesse [8]. These results also represent the most accurate measurements of the diffraction efficiency of which we are aware ($\pm 0.002\%$).

The cavity-finesse method has demonstrated a high sensitivity for measuring the diffraction efficiencies of gratings at the Littrow angle. In addition, we have confirmed that current grating technology can achieve the large aperture size, high diffraction efficiency, and good uniformity that are required for grating interferometers in next-generation gravitational wave detectors.

This research was supported by the NASA grant for the "Modular Gravitational Reference Sensor for Space Gravitational Wave Detection" and by the National Science Foundation (NSF) Stanford LIGO program.

References

1. K.-X. Sun and R. L. Byer, Opt. Lett. **23**, 567 (1998).
2. K.-X. Sun, G. Allen, S. Williams, S. Buchman, D. DeBra, and R. L. Byer, J. Phys.: Conf. Ser. **32**, 137 (2006).
3. S. Traeger, P. Beyersdorf, L. Goddard, E. Gustafson, M. M. Fejer, and R. L. Byer, Opt. Lett. **25**, 722 (2000).
4. P. P. Lu, A. L. Bullington, P. Beyersdorf, S. Traeger, J. Mansell, R. Beausoleil, E. Gustafson, R. L. Byer, and M. M. Fejer, J. Opt. Soc. Am. A **24**, 659 (2007).
5. K.-X. Sun, P. P. Lu, R. L. Byer, J. A. Britten, H. T. Nguyen, J. D. Nissen, C. C. Larson, M. D. Aasen, T. C. Carlson, and C. R. Hoaglan, J. Phys.: Conf. Ser. **154**, 012031 (2009).
6. D. Friedrich, O. Burmeister, A. Bunkowski, T. Clausnitzer, S. Fahr, E.-B. Kley, A. Tünnermann, K. Danzmann, and R. Schnabel, Opt. Lett. **33**, 101 (2008).
7. A. Bunkowski, O. Burmeister, T. Clausnitzer, E.-B. Kley, A. Tünnermann, K. Danzmann, and R. Schnabel, Appl. Opt. **45**, 5795 (2006).
8. *Advanced LIGO Systems Design*, P. Fritshel, ed., LIGO Technical Note LIGO-T010075-01-I (Advanced LIGO Systems Group, 2008).
9. M. D. Perry, R. D. Boyd, J. A. Britten, D. Decker, B. W. Shore, C. Shannon, E. Shults, and L. Li, Opt. Lett. **20**, 940 (1995).
10. B. W. Shore, M. D. Perry, J. A. Britten, R. D. Boyd, M. D. Feit, H. T. Nguyen, R. Chow, G. E. Loomis, and L. F. Li, J. Opt. Soc. Am. A **14**, 1124 (1997).
11. J. A. Britten, W. A. Molander, A. M. Komashko, and C. P. Barty, Proc. SPIE **5273**, 1 (2004).